Supplementary Material

Aggregates of RNA Binding Proteins and ER Chaperones Linked to Exosomes in Granulovacuolar Degeneration of the Alzheimer's Disease Brain

Suppl. Fig. 1

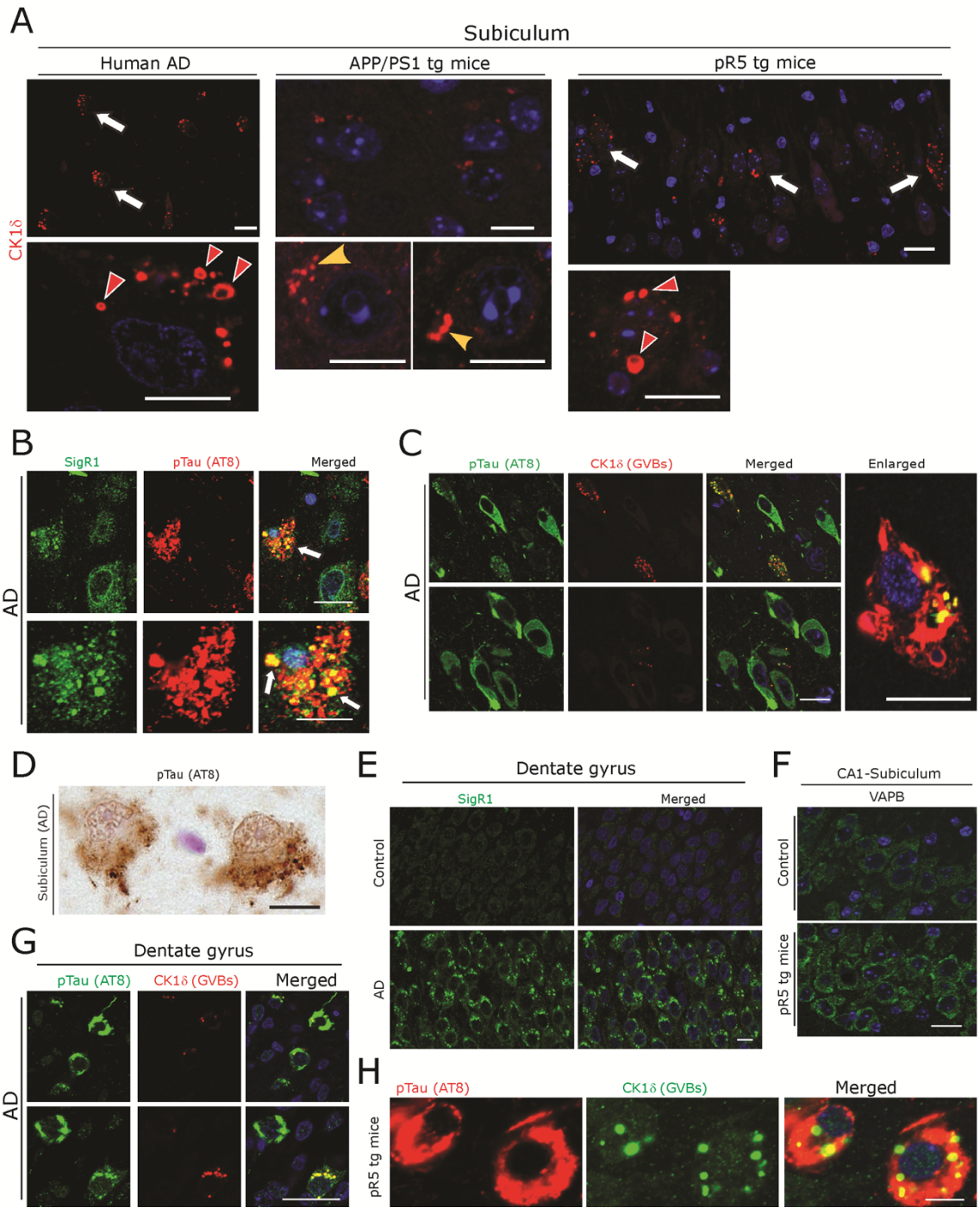

Supplementary Figure 1.
A) Comparison of CK1δ-immunoreactive GVBs (arrows) in AD patient subicular neurons (left panel) versus CK1δ-immunoreactive vesicular structures in APP/PS1 tg (middle panel) and pR5 tg mice CA1-subicular neurons (left panel). Note the mature GVBs with dense core granules and outer layer morphology (red arrow heads) in human AD and in pR5 tg mice compared to incipient GVB-like small granular structures (yellow arrow heads) in APP/PS1 mouse brain. Scale bars: 15 μm.

B) Double immunofluorescence labeling of SigR1 and pTau (AT8). Note the Co-localization of increased SigR1 immunoreactivity (arrows) with granular pTau. Scale bars: 15 μm.

C) Double immunofluorescence labeling for pTau and CK1δ in AD showing neurons with mature pTau tangles do not contain GVBs. Few granular pTau co-localize with GVBs (right panel). Scale bar: 15 μm.

D) DAB immunohistochemistry showing the immunolabelling of pTau in some GVBs. Scale bar: 15 μm.

E) Increased levels of SigR1 in AD patient dentate gyrus neurons (lower panel) compared to control (upper panel). Scale bar: 15 μm.

F) Increased levels of VAPB in pR5 tg mice dentate gyrus neurons. Scale bar: 10 μm.

G) Double immunofluorescence labeling for pTau and CK1δ showing rare GVBs in AD patient dentate gyrus neurons. Scale bar: 15 μm.

H) Double immunofluorescence labeling for pTau and CK1δ showing colocalization in pR5 tg mice CA1-subicular neurons. Scale bar: 15 μm.

Suppl. Fig. 2

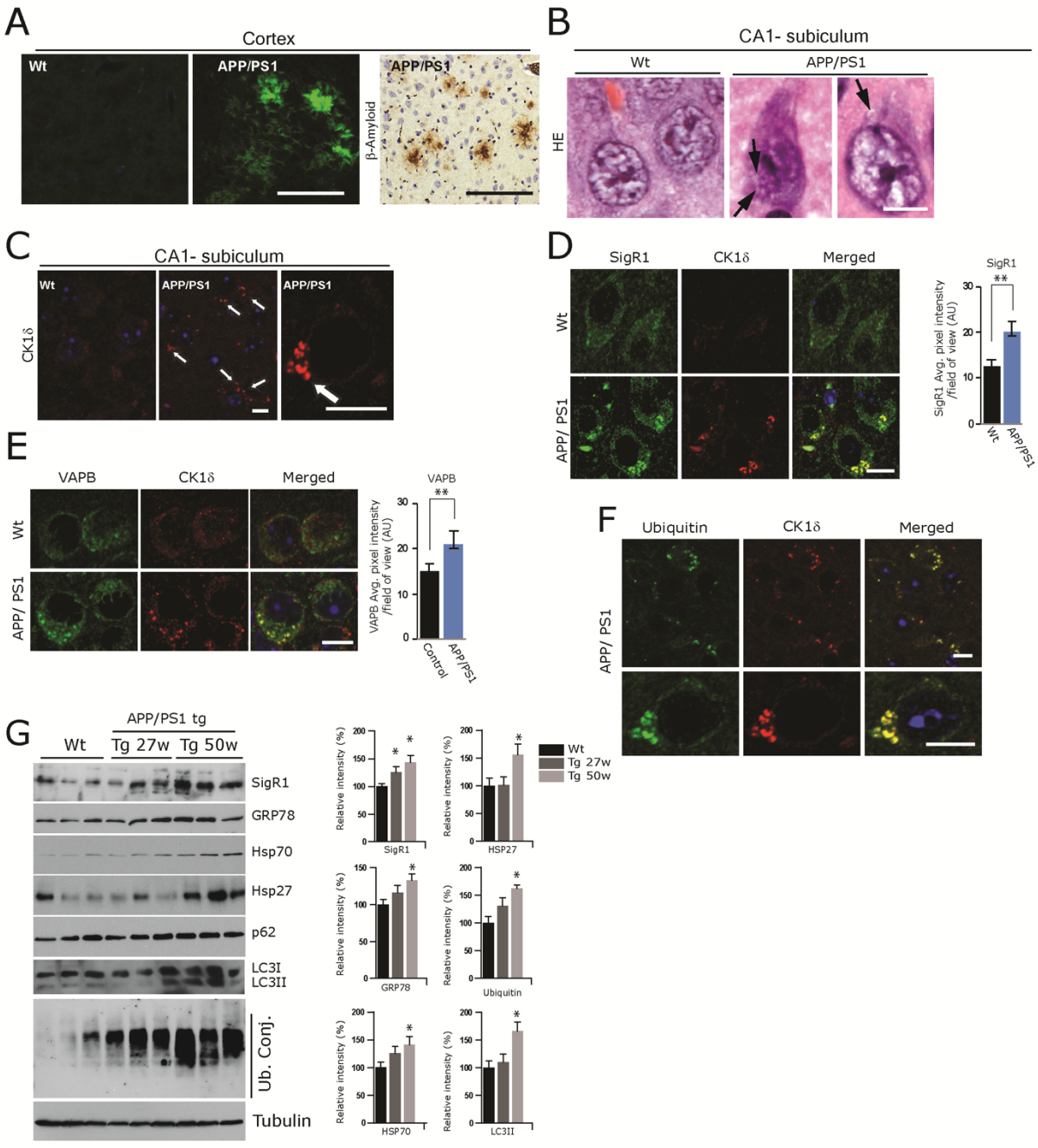
A
Cortex
Wt
APP/PS1
APP/PS1
β-Amyloid
B
CA1- subiculum
Wt
APP/PS1
HE
C
CA1- subiculum
Wt
APP/PS1
APP/PS1
CK1δ
D
SigR1
CK1δ
Merged
Wt
APP/ PS1
SigR1
SigR1 Avg. pixel intensity /field of view (AU)
Wt
APP/PS1
E
VAPB
CK1δ
Merged
Wt
APP/ PS1
VAPB
VAPB Avg. pixel intensity /field of view (AU)
Control
APP/PS1
F
Ubiquitin
CK1δ
Merged
APP/ PS1
G
APP/PS1 tg
Wt
Tg 27w
Tg 50w
SigR1
GRP78
Hsp70
Hsp27
p62
LC3I
LC3II
Ub. Conj.
Tubulin
Wt
Tg 27w
Tg 50w
Relative intensity (%)
SigR1
HSP27
GRP78
Ubiquitin
HSP70
LC3II

Supplementary Figure 2.
A) Thioflavin-S staining (left and middle panel) and Aβ-DAB immunohistochemistry (right panel) showing extracellular plaque pathology in 50 weeks old APP/PS1 tg mouse cortex. Scale bars: 70 μm.

B) Representative H&E stained 50-week-old APP/PS1 tg CA1-subicular neurons compared to age-matched wt mice. Arrows: GVBs like granules. Scale bar: 15 μm.

C) CK1δ-immunoreactivity (arrows) in CA1-subicular neurons of 50-week-old APP/PS1 tg mouse brain compared to the age matched littermate. Enlarged image (right panel) showing groups of CK1δ-immunoreactive vesicles (arrow), probably representing incipient GVBs. Scale bars: 15 μm.

D-F) Double immunofluorescence labeling in CA1-subicular neurons of 50-weeks-old APP/PS1 tg mouse brain for CK1δ together with SigR1 (D), VAPB (E) and Ubiquitin (F), demonstrating co-localization with CK1δ immunoreactive vesicular structures. Note the overall increased immunoreactivities (quantifications) of both SigR1 and VAPB. Scale bars: 15 μm. Values represent the mean ± SD (**$p<0.05$).

G) Immunoblot analysis of total brain homogenates (n=3 for each genotype; wt=50-weeks, APP/PS1 tg mice 27- and 50-weeks) showing an age-dependent increase in ER and proteotoxic stress in APP/PS1 tg mouse brains as demonstrated by elevated levels of the ER chaperone SigR1and GRP78, Hsp70 and Hsp27 and of the ubiquitin conjugates. Right panel: Densitometric quantification of the immunoblots analysis. Values represent the mean ± SD (*$p<0.05$).

Suppl. Fig. 3

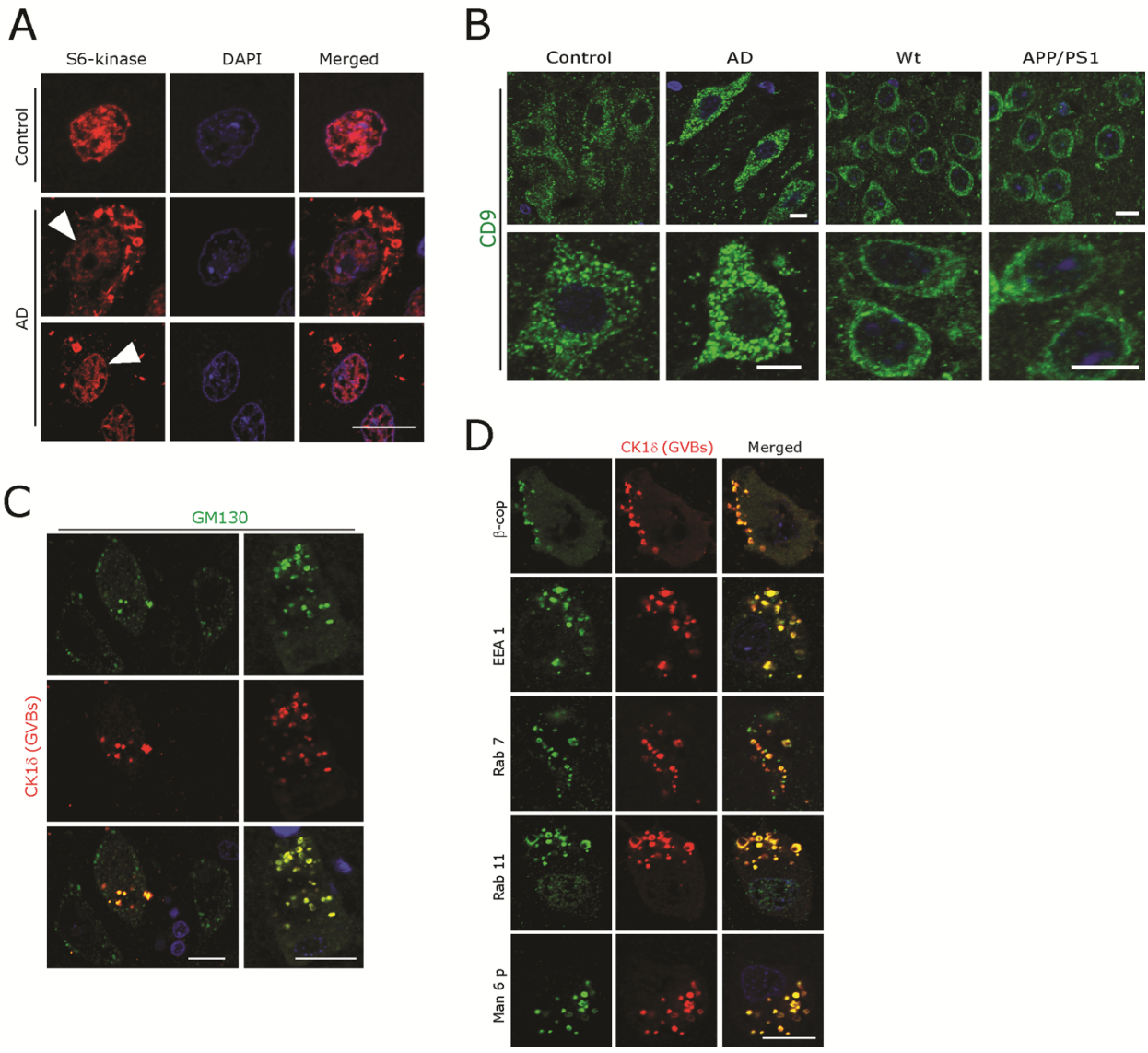

Supplementary Figure 3.
A) Loss of S6-Kinase nuclear immunoreactivity (white arrowheads). Scale bars: 15 µm

B) Immunolabelling of subicular neurons to detect exosomes using tetraspanin CD9 antibody as a proposed marker to label exosomes. Note the widespread CD9 immunoreactivity in human AD and control and in APP/PS1 tg mouse subicular neurons. Scale bars: 15 µm.

C, D) CK1δ immunoreactive GVBs in AD patient show co-localization with the Golgi marker GM130 (C) and with Golgi intermediate (β-cop) as well as early (EEA 1), intermediate (Rab 7) and late (Rab 11, Mannose 6 phosphate) endosomal markers (D). Scale bars: 15 µm.

Supplementary Table 1. List of primary and secondary antibodies used in this study. (Previously used by us in the references: [1-5])

Antibody	Commercial source	Species	Reference	Working Dilution	
				IHC/IF	WB
Primary antibody					
Anti-Amyloid-β (6F/3D)	Leica Biosystems	Mouse	NCL-B-Amyloid	1:50	-
Anti-Amyloid-β (82E1)	IBL	Mouse	10326	1:50	-
Anti-pTau (AT8)	Innogenetics	Mouse	BR-003	1:100	-
Anti-ck1δ (GVBs)	Abcam	Mouse	ab85320	1:100	-
Anti-ck1δ (GVBs)	Abcam	Rabbit	ab151793	1:100	-
Anti-SigR1	Proteintech	Rabbit	15168-1-AP	1:100	-
Anti-SigR1	Santa Cruz	Mouse	Sc-166392	1:50	1:1000
Anti-GRP78 (Bip)	BD Biosciences	Mouse	610978	1:100	1:1000
Anti-HSP27	Cell signalling	Mouse	2402S	-	1:1000
Anti-HSP70	Millipore	Mouse	MAB3516	-	1:1000
Anti-Ubiquitin (ub)	Dako	Rabbit	Z0458	1:100	1:1000
Anti-P62	MBL	Rabbit	PM045	1:200	1:1000
Anti-LC3B	Sigma Aldrich	Rabbit	L7543	1:100	1:1000
Anti-EEA1	BD Biosciences	Mouse	610456	1:100	-
Anti-Rab7	Sigma Aldrich	Mouse	R8779	1:100	-
Anti-Rab 11	Life Technologies	Rabbit	700184	1:100	-
Anti-Mannose- 6PR	Thermo scientific	Mouse	MA1-066	1:100	-
Anti-pTDP43	Cosmo Bio Co. LTD	Mouse	TIP-PTD-M01	1:5000	-
Anti-Matrin3	Bethyl	Rabbit	IHC-00081	1:200	-
Anti-Fus	Novus Biologicals	Rabbit	NB100-2599	1:100	-
Anti-human G3BP	BD Transduction	Mouse	611126	1:100	-
Anti-p70 S6 kinase	Santa Cruz Biotech	Mouse	SC-8418	1:50	-
Anti-GM130	BD Biosciences	Mouse	610822	I:100	-
Anti-VAPB	Home made	Rabbit	-	1:50	-
Anti-β-COP	Thermo scientific	Rabbit	PA1-061	1:100	-
Anti α-Tubulin	Sigma Aldrich	Mouse	T5168	-	1:1000
Anti-Flotillin-1	BD Biosciences	Mouse	610821	1:100	-
Anti-Flotillin-1	Cell signalling	Rabbit	3253S	1:100	-
Anti-CD9	Antibodies online	Rabbit	ABIN6135596	1:100	-
Secondary antibody					
Poly HRP-GAMs/Rb IgG	Immunologic a VWR	Ms/Rb	VWRKDPVB500HRP	Read-to-use	-
Poly HRP-Anti Goat IgG	Immunologic a VWR	Goat	VWRKDPVG110HRP	Read-to-use	-
Biotinylated goat anti-mouse	Vector Laboratories	Goat	BA-9200	1:500	-
Alexa Fluor 488 goat anti-mouse	Life Technologies	Goat	A11001	1:500	-
Alexa Fluor 555 goat anti-mouse	Life Technologies	Goat	A21424	1:500	-
Alexa Fluor 488 goat anti-rabbit	Life Technologies	Goat	A11008	1:500	-
Alexa Fluor 546 goat anti-rabbit	Life Technologies	Goat	A11010	1:500	-

Alexa Fluor 488 donkey anti-goat	Life Technologies	Donkey	A11055	1:500	-
Streptavidin, Alexa Fluor 594 conjugate	Life Technologies	-	S032356	1:500	-
Goat anti-rabbit IgG (H+L), HRP	Thermo Scientific	Goat	31460	-	1:10000
Goat anti-mouse IgG (H+L), HRP	Thermo Scientific	Goat	31430	-	1:10000

REFERENCES

[1] Dreser A, Vollrath JT, Sechi A, Johann S, Roos A, Yamoah A, Katona I, Bohlega S, Wiemuth D, Tian Y, Schmidt A, Vervoorts J, Dohmen M, Beyer C, Anink J, Aronica E, Troost D, Weis J, Goswami A (2017) The ALS-linked E102Q mutation in Sigma receptor-1 leads to ER stress-mediated defects in protein homeostasis and dysregulation of RNA-binding proteins. *Cell Death Differ* **24**, 1655-1671.

[2] Jesse CM, Bushuven E, Tripathi P, Chandrasekar A, Simon CM, Drepper C, Yamoah A, Dreser A, Katona I, Johann S, Beyer C, Wagner S, Grond M, Nikolin S, Anink J, Troost D, Sendtner M, Goswami A, Weis J (2017) ALS-associated endoplasmic reticulum proteins in denervated skeletal muscle: implications for motor neuron disease pathology. *Brain Pathol* **27**, 781-794.

[3] Goswami A, Jesse CM, Chandrasekar A, Bushuven E, Vollrath JT, Dreser A, Katona I, Beyer C, Johann S, Feller AC, Grond M, Wagner S, Nikolin S, Troost D, Weis J (2015) Accumulation of STIM1 is associated with the degenerative muscle fibre phenotype in ALS and other neurogenic atrophies. *Neuropathol Appl Neurobiol* **41**, 304-318.

[4] Vollrath JT, Sechi A, Dreser A, Katona I, Wiemuth D, Vervoorts J, Dohmen M, Chandrasekar A, Prause J, Brauers E, Jesse CM, Weis J, Goswami A (2014) Loss of function of the ALS protein SigR1 leads to ER pathology associated with defective autophagy and lipid raft disturbances. *Cell Death Dis* **12**, 243.

[5] Filezac de L'Etang A, Maharjan N, Cordeiro Brana M, Ruegsegger C, Rehmann R, Goswami A, Roos A, Troost D, Schneider BL, Weis J, Saxena S (2015) Marinesco-Sjogren syndrome protein SIL1 regulates motor neuron subtype-selective ER stress in ALS. *Nat Neurosci* **18**, 227-238.